Korean J. Chem. Eng., 34(2), 470-475 (2017)
DOI: 10.1007/s11814-016-0296-y

pISSN: 0256-1115
eISSN: 1975-7220

Synthesis and characterization of polypyrrole doped by cage silsesquioxane with carboxyl groups

Gang Shi, Youxin Che, Luyan Wu, Yao Rong, and Caihua Ni†

The Key Laboratory of Food Colloids and Biotechnology, Ministry of Education,
School of Chemical and Material Engineering, Jiangnan University, 214122 Wuxi, P. R. China
(*Received 28 May 2015 • accepted 24 October 2016*)

Abstract−Cage silsesquioxane with carboxyl groups (POSS-COOH) was successfully synthesized, after which it was added to polypyrrole (PPy) as a dopant to produce the doped PPy (PPy/POSS-COOH) solution. The PPy/POSS-COOH composites were characterized by FTIR (Fourier transformation infrared spectroscopy), SEM (Scanning electron microscopy), TGA (Thermo-gravimetric analysis), CV (Cyclic voltammetry) and RL (Reflection loss). Compared to PPy without POSS-COOH (un-PPy), the conductivity of PPy/POSS-COOH composites could be improved dramatically, reaching up to 0.850 S/cm at 25 °C. Under N_2 atmosphere, the residual rate of PPy/POSS-COOH was 68% at 700 °C, 14% higher than the one of un-PPy. Meanwhile, PPy/POSS-COOH had a reflection loss below −8 dB over 9.35 to 11.20 GHz, with a minimum value of −10.32 dB at 10.54 GHz, thus demonstrating higher microwave absorption than un-PPy. This method may provide a facile route to produce doped conducting polymers with POSS-COOH.

Keywords: Cage Silsesquioxane, Polypyrrole, Thermal Stability, Electrochemical Activity, Microwave-absorbing Ability

INTRODUCTION

Conducting polymers have attracted considerable attention since being discovered in 1976 [1-3]. Their unique metal-insulator transition induced by doping/de-doping processes, along with their optoelectronic properties controllable through molecular design, attractive mechanical properties and processing advantages have stimulated extensive research into these polymers and their technically relevant applications. This has facilitated the production of different functional devices including organic light emitting diodes [4], electrochromic devices [5,6], field-effect transistors [7,8], integrated circuits [9], supercapacitors [10], photodetectors [11] and sensors [12]. The impact of conducting polymers in the field of electronics is expected to be great, due to their ease of processing, flexibility, light weight and the potential for low-cost device fabrication [9,13]. Polypyrrole (PPy), which is one of the most excellent conducting-polymers, has many advantages, such as non-toxicity, easy synthesis and good chemical stability [14]. However, its low thermomechanical stability and electrochemical activity are major hindrances to industrial application [15,16].

Polyhedral oligomeric silsesquioxane (POSS), an intermediate between silica (SiO_2) and silicone (R_2SiO), is a new class of chemical feedstock for the development of nano-reinforced organic-inorganic hybrid materials [17-20]. $(RSiO_{1.5})_8$, a typical POSS, has a well-defined cage-like framework structure and eight organic groups appended to the vertices of the cage [21]. These organic groups could be further functionalized to produce functional POSS monomers [22,23]. POSS-based composite materials have gradually gathered attention due to the unique structure of POSS monomers [24,25]. Some new routes for the preparation of POSS-polymer composites have been proposed and developed to improve the thermal and mechanical properties of the polymers [26,27], mainly due to the characteristics of organic and inorganic compounds in POSS, while the cage structure also influences the electromagnetic properties [28]. However, there are few reports on experiments combining POSS with functional polymers [29,30].

This article reports that POSS-COOH as a proton dopant has been combined with PPy for the first time. Here, POSS-COOH was prepared by the graft modification of POSS-NH_2 with maleic anhydride (HAM). To study the effect of POSS-COOH on PPy properties, POSS-COOH was combined with PPy. The Si-O cage of POSS-COOH improves the thermal stability of PPy. Simultaneously, the proton of POSS-COOH, as a kind of dopant, enhances the electrochemical activity of PPy. Additionally, the cage-like structure of POSS-COOH would have an impact on the microwave absorption property.

MATERIALS AND METHODS

1. Materials

Iron chloride ($FeCl_3$, 97%) and pyrrole (99.5%) were purchased from Sigma-Aldrich. γ-Aminopropyltriethoxysilane (KH-550) was purchased from Tianyang Chemical Company. N, N-dimethyl formamide and maleic anhydride purchased from National Chemical Groups. All the organic solvents were of analytical grade, and all chemicals were used without any further purification.

2. Synthesis of POSS-NH_2

POSS-NH_2 was prepared as described in the literature [31]. 45 mL of deionized water, 20 mL of anhydrous propanol, 5 mL of acetonitrile and 1 mL of tetraethylammonium hydroxide were mixed

†To whom correspondence should be addressed.
E-mail: nicaihuajnu@yeah.net

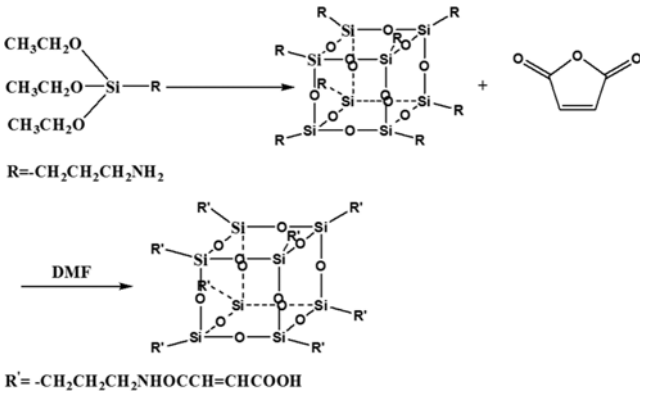

Scheme 1. Synthesis of POSS-NH_2 and POSS-COOH.

in a triple-neck flask equipped with a mechanical stirrer and a condenser. KH-550 (110.5 g) was added to the mixture with vigorous stirring. The solution was allowed to react at 50 °C for 24 hours, resulting in a white crystalline product. The product was washed three times with tetrahydrofuran, and finally it was dried under reduced pressure at 100 °C for 24 hours.

3. Synthesis of POSS-COOH

The POSS-NH_2 thus obtained was dissolved into deionized water. Then, with the molar ratio of 1 : 8, the POSS-NH_2 solution was titrated into the aqueous solution of maleic anhydride. To obtain the product of POSS-COOH aqueous solution, the reaction was continued for eight hours at room temperature.

4. Composition of PPy and POSS-COOH

The pyrrole (0.69 g) was dissolved in 60 mL of deionized water (solution 1) and $FeCl_3$ (0.27 g) was dissolved in 60 mL of deionized water (solution 2). Subsequently, POSS-COOH was added to solution 2 until the pH value of the system was 4.5, 3.5 or 2.5 (solution 3). The solution 2 was then added into solution 3 and stirred in an ice-water bath for eight hours. Finally, the product was washed several times with deionized water until the filtrate was colorless, after which it was dried. The resulting product was a brown green powder.

5. Instruments and Characterization

The structures of the PPy/POSS-COOH were characterized by Fourier transform infrared spectroscopy (FTIR; FTLA 2000, Boman, Canada). The thermal stability was studied by thermogravimetric analysis (TGA/SDTA851e, Mettler Toledo, Switzerland), and the morphology was observed by scanning electron microscope (SEM, JSM-T300, Japan). Elemental analysis was conducted on a Flash EA 1112 microanalyzer. Electrical measurements were performed with a Keithley 6430 SourceMeter remote source meter. The microwave-absorbing measurement was carried out on samples, with the surface area of 15×15 cm^2 and a thickness of 3 mm with an Agilent Network analyzer IIP8720ES.

RESULTS AND DISCUSSION

Fig. 1 shows the infrared spectrum of HAM, POSS-NH_2 and POSS-COOH. The POSS-NH_2 was synthesized under basic conditions by KH-550 [31]. In Fig. 1(a), the peaks at 1,711 cm^{-1} and 2,954 cm^{-1} stand for the stretching vibration of C=O in HAM. A

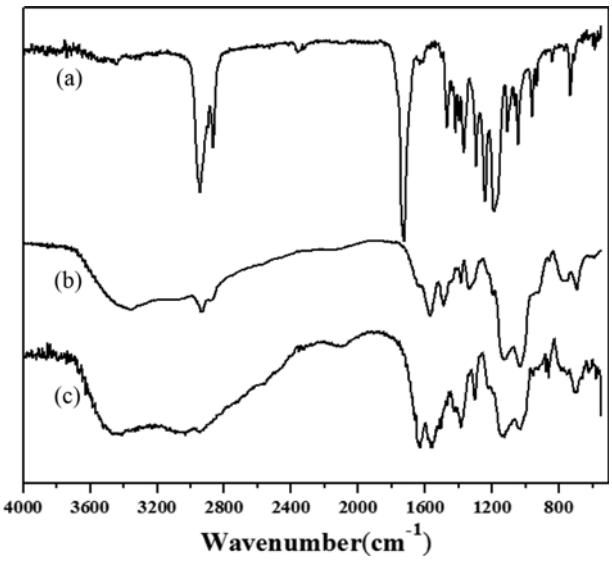

Fig. 1. FTIR spectra of HAM (a), POSS-NH_2 (b) and POSS-COOH (c).

typical FTIR of POSS-NH_2 is shown in Fig. 1(b). The characteristic peaks of the N-H asymmetric stretching vibration and N-H bending vibration can be seen at 3,353 cm^{-1} and 1,553 cm^{-1}, respectively. Meanwhile, the peaks at 1,131 cm^{-1} and 1,025 cm^{-1} are ascribed to Si-O-Si asymmetric stretching vibration [32]. The POSS-COOH was synthesized with POSS-NH_2 and maleic anhydride. From the FTIR of POSS-COOH in Fig. 1(c), two peaks at 3,037 cm^{-1} and 1,640 cm^{-1} emerged apart from those that appear in Fig. 1(b), corresponding to the C=O group of amide and the -OH groups of carboxylic acid, thereby indicating the generation of POSS-COOH. However, the peak of N-H stretching vibration at 3,353 cm^{-1} in Fig. 1(c) shows that not all amino groups at the eight vertices of POSS-NH_2 were reacted with HAM, due to significant steric hindrance of POSS-NH_2.

When PPy was doped by the proton of POSS-COOH, the two

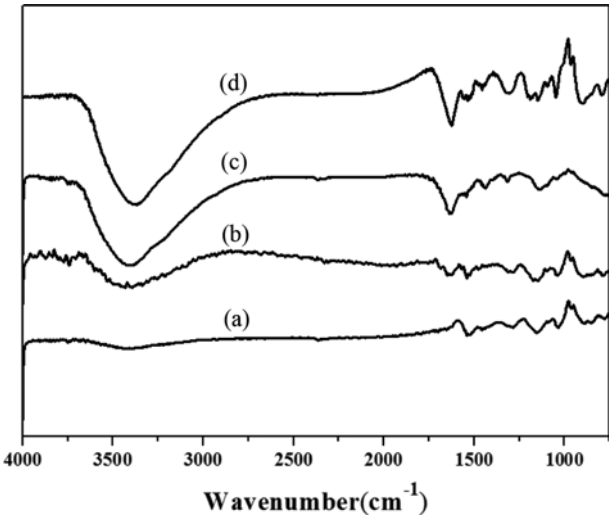

Fig. 2. FTIR spectra of un-PPy (a) and PPy/POSS-COOH with pH= 4.5 (b), pH=3.5 (c) and pH=2.5 (d).

Table 1. Elemental analysis (EA) of un-PPy and PPy/POSS-COOH with pH=4.5, pH=3.5 and pH=2.5

	N (%)	C (%)	H (%)	Si+O (%)
Un-PPy	13.8%	75.7%	6.86%	3.57%
PPy/POSS-COOH (pH=4.5)	15.0%	59.7%	5.99%	19.1%
PPy/POSS-COOH (pH=3.5)	13.9%	56.5%	5.94%	23.5%
PPy/POSS-COOH (pH=2.5)	10.1%	51.3%	4.90%	33.5%

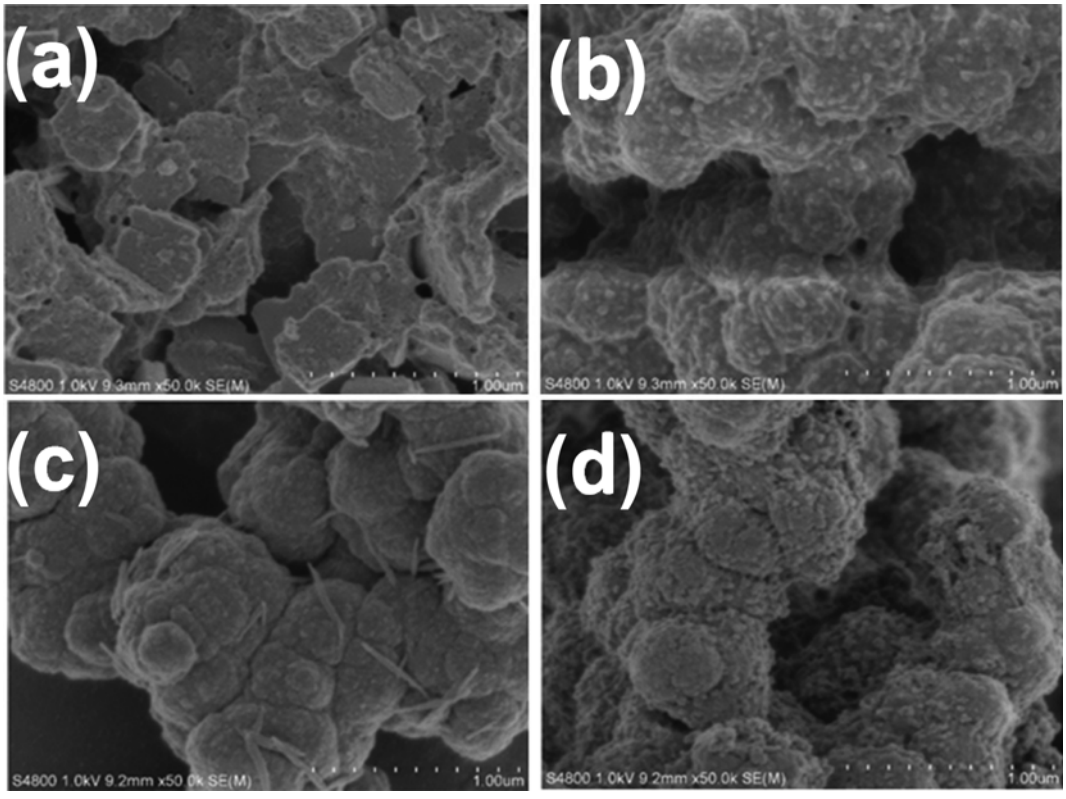

Fig. 3. SEM of un-PPy (a) and PPy/POSS-COOH with pH=4.5 (b), pH=3.5 (c) and pH=2.5 (d).

compounds could be combined with each other through ionic bonding. Fig. 2 displays the FTIR of PPy without POSS-COOH (un-PPy) and PPy doped by POSS-COOH (PPy/POSS-COOH) with different pH values. The FTIR spectra of un-PPy can be seen in Fig. 2(a), in which the peak at 1,544 cm^{-1} stands for the stretching vibration of the pyrrole ring. The peaks at 1,229 cm^{-1} and 1,159 cm^{-1} are ascribed to C-H in-plane deformation vibration, and the peaks at 891 cm^{-1} and 778 cm^{-1} are attributed to C-H plane bending vibration. Fig. 2(b), 2(c) and 2(d) stand for the FTIR spectra of PPy/POSS-COOH with pH=4.5, 3.5 and 2.5, respectively, and some new peaks emerged in comparison to Fig. 2(a). The peak of 1,624 cm^{-1} is ascribed to C=O, and the Si-O-Si stretching vibration peaks can be seen at 1,133 cm^{-1} and 1,082 cm^{-1}, which demonstrate that PPy was doped successfully by POSS-COOH. The effect of pH value of POSS-COOH on PPy can be seen by contrasting Fig. 2(b), 2(c) and 2(d). With the pH value decreasing, the peaks at 1,624 cm^{-1}, 1,133 cm^{-1} and 1,082 cm^{-1} become increasingly stronger, demonstrating that the dopant amount of POSS-COOH has gradually increased.

Table 1 displays the elemental analyses (EA) of un-PPy and PPy/POSS-COOH with pH=4.5, 3.5 and 2.5. In contrast to un-PPy, PPy/POSS-COOH processes a lower proportion of N, C and H but a higher proportion of the Si and O, indicating that PPy was successfully doped with POSS-COOH. Simultaneously, the proportion of the Si and O increased with the reduction of pH value, suggesting that PPy was doped by more POSS-COOH. This is like the tendency reported in the above-mentioned FTIR tests.

Fig. 3 presents the SEM (Scanning electron microscope) images of the un-PPy (a) and PPy/POSS-COOH with pH=4.5 (b), 3.5 (c) and 2.5 (d). The morphology of un-PPy is similar to sheet, as seen in Fig. 3(a). However, the morphology of the PPy/POSS-COOH changed significantly and thereby developed hierarchical structures (nano/micro-structures). From Fig. 3(b) to 3(d), the density of nanoparticles on the micro-structures increased with the decreasing of pH value, which is consistent with the increasing mass of POSS-COOH. When PPy was doping with POSS-COOH, the carboxyl groups at the eight vertices of POSS and the N on the chain of the PPy interacted with each other through the ionic bond and self-assembled into PPy/POSS-COOH nanoparticles (as seen in Scheme 2). Nanoparticles were increased with the decrease of pH,

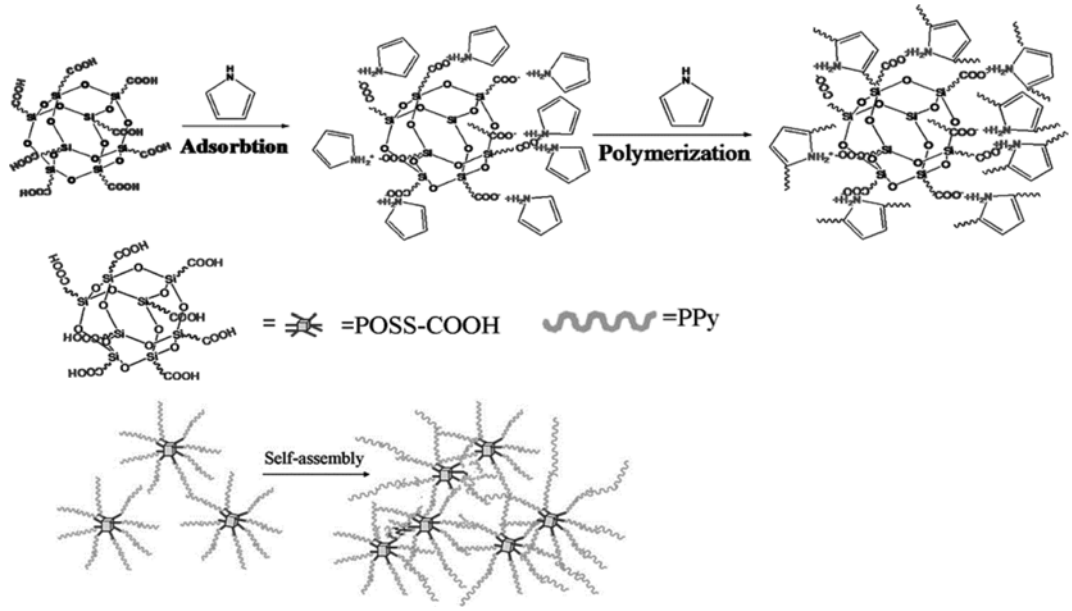

Scheme 2. The growth mechanism of the PPy/POSS-COOH.

which was consistent with the element analysis of POSS content. High-density nanoparticles on the micro-structures make for the enhanced specific surface area of PPy, which could affect some properties of PPy, such as capability, sensing property and so on. When pH=2.5, most of the nanoparticles were produced on the micro-structures, as shown in Fig. 3(d).

Thermo-gravimetric analysis (TGA) is an effective way to characterize the thermal stability of a material. The TGA curves of un-PPy and PPy/POSS-COOH with pH=4.5, 3.5 and 2.5 are displayed in Fig. 4. In the case of un-PPy, TGA shows that the initial weight loss from 100 °C to 250 °C is caused by water vaporization (as shown in Fig. 4(a)). Meanwhile, the weightlessness of PPy/POSS-COOH from 100 °C to 250 °C is due to the water vaporization and the decomposition of organic groups at vertices of POSS-COOH (as shown in Fig. 4(b), 4(c) and 4(d)). From 250 °C to 700 °C, The TGA curves of all samples have no significant weight-loss peak and decline slowly, due to the slow decomposition of PPy chains. At 700 °C, the residual rates of un-PPy and PPy/POSS-COOH at pH=4.5, 3.5 and 2.5 are 54%, 59%, 63% and 68%, respectively. The results suggest that the thermal stability of PPy/POSS-COOH was higher than that of the un-PPy, and that the thermal stability of PPy/POSS-COOH gradually increased along with the decrease of pH value. Therefore, the results could be explained by the nano effect of the POSS and the fact that the POSS framework was highly heat-resistant. The bonding energy of Si-O (451.4 kJ/mol) was much higher than that of C-C (355.3 kJ/mol). Hence, it was more difficult for the sample with high content of POSS-COOH to be thermally decomposed than one with low content of POSS-COOH. Especially, the residual rate of PPy/POSS-COOH composite with pH=2.5 is 68% at 700 °C, which is 14% higher than the one of un-PPy. Therefore, that could be explained by the nano effect of the POSS and the fact that the POSS framework had high heat resistance property.

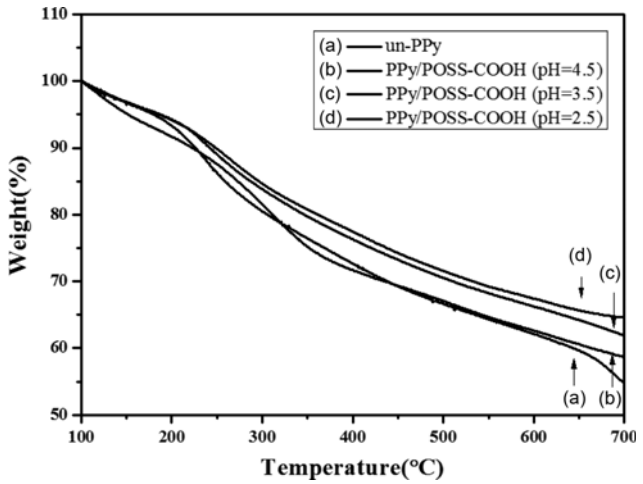

Fig. 4. TGA of un-PPy (a) and PPy/POSS-COOH with pH=4.5 (b), pH=3.5 (c) and pH=2.5 (d).

The un-PPy and PPy/POSS-COOH were compacted into plastic containers with 1 cm in diameter and 1 cm in height, the resistance of which was measured with a multimeter. The conductivity (σ) of the above-mentioned samples was calculated according to the formula σ=L/RS (where L is the length of the resistor, R is the

Table 2. Conductivity of un-PPy and PPy/POSS-COOH with pH=4.5, pH=3.5 and pH=2.5

	Un-PPy	PPy/POSS-COOH (pH=4.5)	PPy/POSS-COOH (pH=3.5)	PPy/POSS-COOH (pH=2.5)
POSS(Si+O) wt%	0	14.9%	19.2%	29.3%
Conductivity (S/cm)	3.16×10^{-10}	2.18×10^{-4}	5.45×10^{-3}	0.850

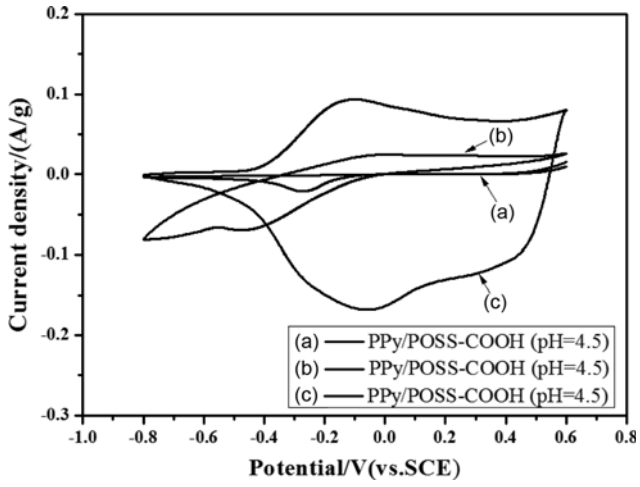

Fig. 5. C-V curves of PPy/POSS-COOH with pH=4.5 (a), pH=3.5 (b) and pH=2.5 (c).

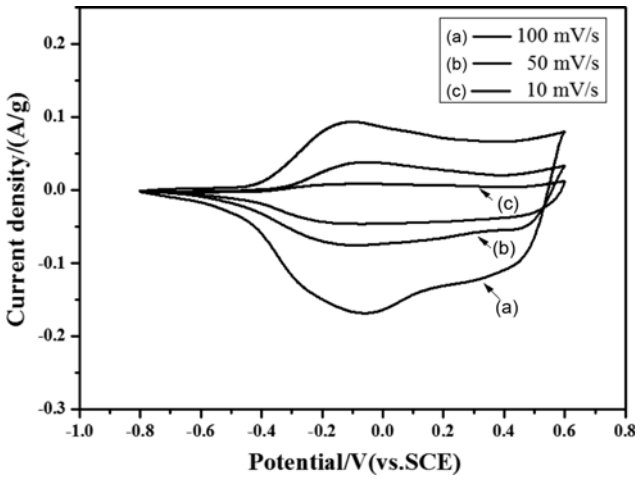

Fig. 6. C-V curves of PPy/POSS-COOH with pH=2.5 electrode at various scan rates.

resistance and S is the sectional area of the resistor). Table 2 shows that the conductivity of un-PPy and PPy/POSS-COOH (pH=4.5, 3.5 and 2.5) are 3.16×10^{-10} S/cm, 2.18×10^{-4} S/cm, 5.45×10^{-3} S/cm and 0.850 S/cm, respectively. And the conductivity of the samples increases with the decrease of pH value due to the enhanced percentage of the dopant POSS-COOH. In the case of higher percentage of dopant, the PPy has more protons and higher specific surface area, making for higher conductivity. For example, the conductivity of the PPy doped with 29.3% of POSS-COOH (pH=2.5) is 0.850 S/cm, which is much higher than that of the traditional PPy (0.005 S/cm) [33].

Cyclic voltammetry (CV) measurements in 1 M H_2SO_4 electrolyte at a scan rate of 100 mv s^{-1} were performed at the potential window from −0.8 to 0.6 V versus SCE. Fig. 5(a)-5(c) stand for the CV results of PPy/POSS-COOH composites with pH=4.5, 3.5 and 2.5, respectively. Fig. 5(a) and 5(b) show irregular and weak redox peaks, indicating that PPy/POSS-COOH composites with higher pH value have poor electrochemical activity. However, in Fig. 5(c) PPy/POSS-COOH at pH=2.5 has regular and strong redox peaks at −0.2 V and −0.15 V with perfect symmetry. Especially, the oxidation peak current density and the reduction peak current density of it are 0.093 A/g and −0.17 A/g, respectively, thus demonstrating that PPy/POSS-COOH composites with lower pH values have good electrochemical activity. The electrochemical activity of PPy/POSS-COOH composites was mainly affected by the quantity of POSS-COOH, which is crucial to the dopant quantity of the proton and the specific surface area of composites. More protons and higher specific surface area would lead to the greater electrochemical activity of composites. The PPy/POSS-COOH with a high pH value has a small quantity of protons, which is difficult to supply PPy (incomplete doping), thereby resulting in the poor electrochemical activity. The dopant of POSS-COOH at different pH values mainly influences the morphology of composites (as shown in Fig. 3). The high specific surface area of PPy/POSS-COOH with pH=2.5 (Fig. 3(d)) increases the electrode/electrolyte contact area and shortens the path lengths for electronic or electrolyte ion transport, which is valuable to enhance the utilization of active materials.

To test the electrochemical stability of the PPy/POSS-COOH with pH=2.5, CV measurements at different scan rates from 5 to 500 mV s^{-1} were recorded. Apparently, in Fig. 6 each curve has the same form and the total current increases with increasing scan rates. Especially, the redox peaks maintain good symmetry at high scan rates, indicating good electrochemical stability of the composite, as shown in Fig. 6(a). Accordingly, the cage POSS-COOH had good mechanical performance that limited the swelling and compression of doped PPy through the redox process, and then reduced the decomposition of PPy.

Conducting polymer is a kind of dielectric loss absorbing material [34]. Particularly, the microwave absorption of the conducting polymer increases with the increase in composite conductivity (σ) as $10^{-9}<\sigma<10^{0}$ S/cm [35]. As described in the aforementioned characterization, the PPy/POSS-COOH has the highest conductivity at pH=2.5, so it was chosen as the sample for discussion. The microwave absorption of the composite was investigated over the frequency range of 7-13.5 GHz using a microwave vector network

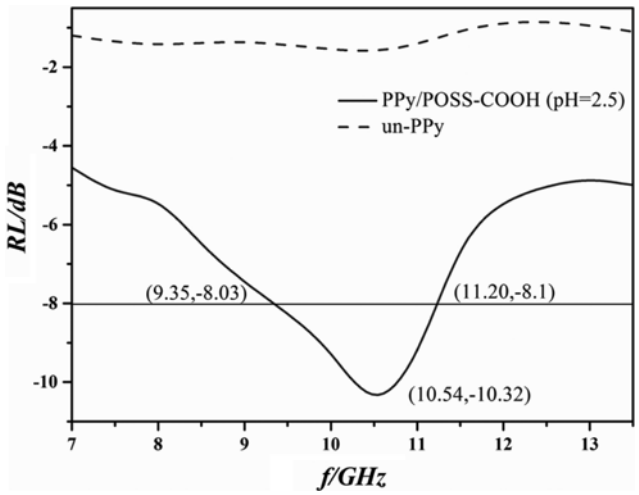

Fig. 7. RL curves of un-PPy and PPy/POSS-COOH with pH=2.5.

analyzer. Fig. 7 shows the reflection loss (RL) curves of the un-PPy and PPy/POSS-COOH with pH=2.5. Compared with the un-PPy, PPy/POSS-COOH composites showed higher microwave absorption (lower RL). There were more protons in the PPy/POSS-COOH composites with pH=2.5, so the dielectric performance is that of higher electrical conductivity, leading to higher microwave absorption. Meanwhile, the cage-like framework structure of POSS enhances equivalent polarization rate of composition, which could contribute to the improvement of microwave absorption.

CONCLUSIONS

POSS-COOH was prepared successfully through graft modification. Moreover, it was the first time that POSS-COOH was combined with PPy as a dopant. Compared to un-PPy, the thermal stability, electrochemical activity and microwave-absorbing ability of PPy/POSS-COOH composites are enhanced.

ACKNOWLEDGEMENTS

This work was supported by the Jiangsu Province Science Foundation for Youths (BK20140158), the National Basic Research Program (21401079, 21501069), Research Fund for the Doctoral Program of Higher Education (20130093120003), Fundamental Research Funds for the Central Universities (JUSRP51626B).

REFERENCES

1. H. Shirakawa, *Angew. Chem. Int. Ed.*, **40**, 2575 (2001).
2. A. G. MacDiarmid, *Angew. Chem. Int. Ed.*, **40**, 2581 (2001).
3. A. J. Heeger, *Angew. Chem. Int. Ed.*, **40**, 2591 (2001).
4. J. H. Burroughes, D. D. C. Bradley, A. R. Brown, R. N. Marks, K. Mackay, R. H. Friend, P. L. Burns and A. B. Holmes, *Nature*, **347**, 539 (1990).
5. G. Sonmez, H. B. Sonmez, C. K. E. Shen and F. Wudl, *Adv. Mater.*, **16**, 1905 (2004).
6. G. Sonmez, C. K. F. Shen, Y. Rubin and F. Wudl, *Angew. Chem. Int. Ed.*, **43**, 1498 (2004).
7. F. Garnier, R. Hajlaoui, A. Yassar and P. Srivastava, *Science*, **265**, 1684 (1994).
8. J. Z. Wang, Z. H. Zheng, H. W. Li, W. T. S. Huck and H. Sirringhaus, *Nat. Mater.*, **3**, 171 (2004).
9. C. J. Drury, C. M. J. Mutsaers, C. M. Hart, M. Matters and D. M. de Leeuw, *Appl. Phys. Lett.*, **73**, 108 (1998).
10. M. Selvakumar, and S. Pitchumani, *Korean J. Chem. Eng.*, **27**, 977 (2010).
11. G. Yu, C. Zhang and A. J. Heeger, *Appl. Phys. Lett.*, **64**, 1540 (1994).
12. G. Shi, L. Q. Li, L. X. Liu, D. R. Xu, N. Lu, J. Y. Hao, C. Y. Huang and L. F. Chi, *J. Mater. Chem.*, **22**, 12096 (2012).
13. I. Kymissis, C. D. Dimitrakopoulos and S. Purushothaman, *J. Vac. Sci. Technol. B*, **20**, 956 (2002).
14. A. Rudge, I. Raistrick, S. Gottesfeld and J. P. Ferraris, *Electrochim. Acta*, **39**, 273 (1994).
15. Y. Z. Li, Q. H. Zhang, X. Zhao, P. P. Yu, L. H. Wu and D. J. Chen, *J. Mater. Chem.*, **22**, 1884 (2012).
16. V. Khomenko, E. Frackowiak and F. Beguin, *Electrochim. Acta*, **50**, 2499 (2005).
17. J. D. Lichtenhan, *Comments Inorg. Chem.*, **17**, 115 (1995).
18. H. Honarkar, M. Barmar, M. Barikani and P. Shokrollahi, *Korean J. Chem. Eng.*, **33**, 319 (2016).
19. W. A. Zhang and A. H. E. Muller, *Prog. Polym. Sci.*, **38**, 1121 (2013).
20. Z. H. Li, D. C. Wu, Y. R. Liang, R. W. Fu and K. Matyjaszewski, *J. Am. Chem. Soc.*, **136**, 4805 (2014).
21. C. H. Ni, G. F. Ni, L. P. Zhang, J. Q. Mi, B. L. Yao and C. P. Zhu, *J. Colloid Interf. Sci.*, **362**, 94 (2011).
22. C. H. Ni, G. J. Zhu, C. P. Zhu, B. L. Yao and D. N. T. Kumar, *Colloid Polym. Sci.*, **288**, 1193 (2010).
23. K. Wu, L. Song, Y. Hu, H. D. Lu, B. K. Kandola and E. Kandare, *Prog. Org. Coat.*, **65**, 490 (2009).
24. G. Z. Li, L. C. Wang, H. L. Ni and C. U. Pittman, *J. Inorg. Organomet. P.*, **11**, 123 (2001).
25. M. Opanasenko, W. O. Parker, M. Shamzhy, E. Montanari, M. Bellettato, M. Mazur, R. Millini and J. Cejka, *J. Am. Chem. Soc.*, **136**, 2511 (2014).
26. S. H. Phillips, T. S. Haddad and S. J. Tomczak, *Curr. Opin. Solid St. M. Sci.*, **8**, 21 (2004).
27. C. H. Ni, G. Wu, C. P. Zhu and B. L. Yao, *J. Phys. Chem. C*, **114**, 13471 (2010).
28. Q. F. Li, Y. H. Xu, J. S. Yoon and G. X. Chen, *J. Mater. Sci.*, **46**, 2324 (2011).
29. M. Ak, B. Gacal, B. Kiskan, Y. Yagci and L. Toppare, *Polymer*, **49**, 2202 (2008).
30. K. Wang, X. Guan, S. Chai, Q. Zou, X. Zhang and J. Zhang, *Biosens. Bioelectron.*, **64**, 94 (2015).
31. Z. Zhang, G. Liang and T. Lu, *J. Appl. Polym. Sci.*, **103**, 2608 (2007).
32. F. J. Feher, D. A. Newman and J. F. Walzer, *J. Am. Chem. Soc.*, **111**, 1741 (1989).
33. B. Dong, D. Y. Zhong, L. F. Chi and H. Fuchs, *Adv. Mater.*, **17**, 2736 (2005).
34. R. Iqbal, M. K. Khosa, M. A. Jamal and M. Hamid, *Korean J. Chem. Eng.*, **32**, 362 (2015).
35. Z. Z. Wang, H. Bi, J. Liu, T. Sun and X. L. Wu, *J. Magn. Magn. Mater.*, **320**, 2132 (2008).